Available online at www.sciencedirect.com
ScienceDirect
Journal of Hazardous Materials 158 (2008) 557–567
Journal of Hazardous Materials
www.elsevier.com/locate/jhazmat

Simultaneous removal of metal ions and linear alkylbenzene sulfonate by combined electrochemical and photocatalytic process

H.D. Doan [a,*], M. Saidi [b]

[a] *Department of Chemical Engineering, Ryerson University, 350 Victoria Street, Toronto, Ont., Canada M5B 2K3*
[b] *Environment Canada, Toronto, Ont., Canada*

Received 27 October 2007; received in revised form 29 January 2008; accepted 30 January 2008
Available online 8 February 2008

Abstract

Combined electrochemical removal of Zn^{++} and Ni^{++} and photo-oxidation of linear alkylbenzene sulfonate (LAS) by suspended TiO_2 particles was investigated. The effect of different process variables such as current density, pH and liquid flow rate on the sole electrochemical reduction of metal ions was also evaluated. At pH of 5.0, the removal of Zn^{++} increased by 28% with increases in the liquid flux from 0.0021 to 0.0172 $m^3\ m^{-2}\ s^{-1}$ while the removal of Ni^{++} was only enhanced marginally. Under optimum operating conditions used in the present study (liquid flux = 0.0172 $m^3\ m^{-2}\ s^{-1}$, current density = 0.166 mA cm^{-2}, pH 5.0 and in the presence of LAS), Zn^{++} and Ni^{++} were reduced by 86 and 56%, respectively, over 7 h of the sole electrochemical treatment. For the sole photocatalytic treatment of LAS at pH of 5.0, a 60% LAS degradation was obtained. However, the liquid flow rate did not have any considerable effect on the LAS oxidation. Finally, in the combined photocatalytic–electrolytic process, the LAS degradation increased to 76%. Nonetheless, in the combined system the Zn^{++} and Ni^{++} removal remained at comparable levels to those obtained in the sole electrochemical system.

Keywords: Electrochemical; Photocatalytic; LAS; Ni^{++}; Zn^{++}

1. Introduction

In the present study, a combined photocatalytic and electrochemical method was developed and assessed for treating wastewater from an electro-coating process, which contained both heavy metals and organic compounds. In the electro-coating (e-coat) process an electrical current is used to deposit paint onto metal parts immersed in a paint bath. Due to the uniformity of the applied coating and its excellent adhesion, the electro-coating process offers a good corrosion protection on both steel and aluminum substrates. However, a large volume of wastewater is generated during the electro-coating process from different stages containing various toxic heavy metals and organic compounds. Rinse water from a pretreatment unit in e-coat usually contains Zn^{++} and Ni^{++} at about 20 ppm [1]. Chemical precipitation is a conventional method that is widely used in industry to remove metal ions in wastewaters. For some metals, such as Zn^{++} and Ni^{++}, this conventional method is sufficient for compliance to the allowable limits for treated water discharge [2,3]. However, hydroxide precipitation requires extensive use of various chemicals. The major drawback of this technique is the generation of a large amount of sludge that required further treatment and landfill. Further costly treatment of the sludge prior to landfill and its negative environmental impact make this method undesirable.

Metal ions can be removed from an aqueous solution by electrodeposition. This technique has a low sludge production, a low start-up and operating cost, and no chemical contamination of the treated water. Electrochemical reactions can be carried out at ambient pressure and temperature and can be easily terminated by disconnecting the cell current.

Additionally, the wastewater from an electro-coating plant contains some organics, which are used in various stages of the process. In the pretreatment stage, some organic compounds are used for the cleaning of metallic parts. Surface-active agents or surfactants are used widely as cleaning agents. Many surfactants are not biodegradable, or their biodegradation is very slow [4]. Linear alkylbenzene sulfonate (LAS) and sodium dodecylbenzene sulfonate (DBS) are the most common anionic surfactants used in domestic and industrial detergents. LAS is

* Corresponding author. Tel.: +1 416 979 5000x6341; fax: +1 416 979 5083.
E-mail address: hdoan@ryerson.ca (H.D. Doan).

0304-3894/$ – see front matter © 2008 Elsevier B.V. All rights reserved.
doi:10.1016/j.jhazmat.2008.01.102

Nomenclature

A	electrode area (m^2)
C	LAS concentration in the solution at a given time ($mg\,L^{-1}$)
C_M	concentration of metal ions in the solution at a given time ($mg\,L^{-1}$)
C_{Mo}	initial concentration of metal ions in the solution ($mg\,L^{-1}$)
C_o	initial LAS concentration in the solution ($mg\,L^{-1}$)
COD	chemical oxygen demand ($mg\,L^{-1}$)
COD_0	initial chemical oxygen demand ($mg\,L^{-1}$)
C_S	concentration of metal ions at the surface of the cathode ($mg\,L^{-1}$)
D_{AB}	diffusivity of metal ions in liquid ($m^2\,s^{-1}$)
E^o	standard half-cell potential (V)
J_D	J factor for mass transfer ($J_D = Sh/[Re{\cdot}Sc^{1/3}]$)
k	rate constant for first-order kinetics of metal removal (h^{-1})
k_c	mass transfer coefficient for metal ions ($m\,h^{-1}$)
k_r	rate constant for first-order kinetics of LAS removal (h^{-1})
K	equilibrium constant of organic adsorption ($L\,mg^{-1}$)
L	characteristic length (hydraulic diameter of the opened-channel electrochemical cell in the present study) (m)
Re	the Reynolds number ($Re = [L{\cdot}\rho{\cdot}u]/\mu$)
Sh	the Sherwood number ($Sh = [k_c{\cdot}L]/D_{AB}$)
Sc	the Schmidt number ($Sc = \mu/[\rho{\cdot}D_{AB}]$)
t	time (h)
u	superficial liquid velocity ($m\,s^{-1}$)
V	liquid volume (m^3)
Greek symbols	
μ	liquid viscosity ($kg\,m^{-1}\,s^{-1}$)
ρ	liquid density ($kg\,m^{-3}$)

more biodegradable than DBS since its alkyl portion is not branched. However, it has been reported that LAS is a recalcitrant at a high concentration of 3000 $mg\,L^{-1}$; hence, it does not respond to biological treatments [5]. Different methods have been employed to treat surfactants, such as: biological treatment, adsorption, flocculation and coagulation, and advanced oxidation. In an adsorption process, undesirable sludge is produced, which needs further treatment. Biological treatments are very economical compared to other methods; however, for refractory and non-biodegradable compounds, these techniques are ineffective.

Advanced oxidation processes (AOPs) are promising methods for the treatment of non-biodegradable organics. One of the popular AOPs is UV/TiO_2 photocatalysis. In photocatalysis, the pollutants are degraded by a metal oxide semiconductor such as titanium dioxide, acting as the photocatalyst, in the presence of UV light. The photocatalyst help producing highly reactive intermediates, mainly hydroxyl radicals, capable of oxidizing almost all organic pollutants.

For a wastewater containing both metal ions and organic compounds, an electrochemical cell alone can only remove metal ions but it may not be capable of achieving complete degradation of organic compounds in the wastewater. On the other hand, a photocatalytic cell alone can degrade organics effectively while it leaves metal ions with fairly negative standards reduction potentials such as Zn^{++} and Ni^{++} in solution. The development of an effluent treatment technique, which could degrade organic pollutants and simultaneously remove metal ions from wastewaters, would thus be of benefit to industry. The objective of this study was thus to investigate the feasibility of a combined electrochemical and photocatalytic system for the treatment of a simulated wastewater containing both metal ions and LAS.

2. Experimental methodology

2.1. Materials and analytical methods

Linear alkylbenzene sulfonate was used as a model organic compound. Molecular structure of LAS is shown below where R represent alkyl chain ($R = (CH_2)_{11}CH_3$).

Degussa P25 TiO_2 (mainly anatase with surface area 55 $m^2\,g^{-1}$) was used as a photocatalyst in the present study. The concentration of suspended titanium dioxide in aqueous solutions used in all experiments was kept at 1 $g\,L^{-1}$. For experiments with immobilized TiO_2, granular silica gel (grade 40, 6–12 mesh, Sigma–Aldrich) was used as a supporting material for TiO_2 immobilization.

Nickel sulfate hexahydrate and zinc sulfate heptahydrate were used to prepare the simulated wastewater containing 20 ppm Zn^{++} and 20 ppm Ni^{++}. Potassium sulfate was also added to the solution as a supporting electrolyte (250 ppm). Water samples were taken from the experimental set-up at preset intervals and metal ion concentrations in the solutions were measured using atomic absorption spectrophotometer (AAnalyst 800, PerkinElmer, Toronto, Ontario, Canada).

Analytical measurement of LAS was carried out based on the standard method for the determination of an anionic surfactant that acts as a methylene blue active substance (MBAS) [6]. MBAS (surfactant) brings about the transfer of methylene blue, a cationic dye, from an aqueous solution into an immiscible organic liquid by an ion pair formation of the MBAS anion and the methylene blue cation. The intensity of the blue color formed in the organic solvent (chloroform) is a measure of the amount of the methylene blue active substance (surfactant) present in the water sample. The blue color in the chloroform was read at 652 nm using a UV/visible spectrophotometer (Pharmacia LKB-Ultrospec III, LabEquip Ltd., Markham, Ontario).

To prepare methylene blue reagent, 100 mg of methylene blue was dissolved in distilled water and diluted to 100 mL in a volumetric flask. Thirty milliliters of this solution, 500 mL of water,

41 mL of H_2SO_4 6N, and 50 g $NaH_2PO_4{\cdot}H_2O$ were added to 1000 mL volumetric flask, dissolved thoroughly and diluted to 1000 mL with distilled water. To make wash solution, 41 mL of H_2SO_4 6N was added to 500 mL of distilled water. Fifty grams of $NaH_2PO_4{\cdot}H_2O$ was added to the solution, dissolved thoroughly and diluted to 1000 mL with distilled water.

Standard LAS solutions were prepared by diluting an appropriate amount of LAS with distilled water. The LAS concentration of 100 mg L^{-1} was used in all experiments. The following procedure was used to extract LAS from wastewater samples taken from the experimental set-up. Ten-milliliters water sample was centrifuged and filtered through a 934-AH Whatman glass microfiber filter paper to remove TiO_2 particles. Two milliliters of the centrifuged water sample was taken and diluted appropriately so that the measured concentration of LAS would be less than 2 mg L^{-1}. Ten milliliters of the diluted sample was added to a clean 14 mL centrifuge tube and one drop of phenolphthalein indicator solution was added to the sample and mixed. NaOH 1N was added to make the solution alkaline (solution became pink) and then H_2SO_4 1N was added until the pink color disappeared and the solution became slightly acidic. 1 mL of chloroform, $CHCl_3$, and 2.5 mL of methylene blue reagent were added to the tube and the tube was shaken vigorously for 30 s. The aqueous solution (raffinate) was removed and transferred to another tube. The tube containing chloroform was capped to prevent losses. The extraction procedure was repeated two more times with the aqueous raffinate. Five milliliters of the wash solution was added to all of the combined $CHCl_3$ extracts, shaken vigorously for 30 s, and then allowed to be separated. The wash solution raffinate was extracted two times by chloroform, 1 mL each time. Finally all chloroform extracts were combined and diluted using chloroform to 10 mL. The absorbance at 652 nm was measured against $CHCl_3$ blank by UV spectrophotometer. Standard curve was prepared by measuring the absorbance of the standard solutions in the range of 0–150 mg LAS/L. The extraction procedure for standard solution was also the same as described above.

The amount of chemical oxygen demand (COD) of the wastewater samples was measured using the standard COD test [6]. Water samples were periodically taken from the effluent of the reactor and centrifuged to remove suspended solids. 2.5 mL aliquots of the clear supernatants of the water samples were used for the COD tests.

2.2. Immobilization of TiO_2

Commercial Degussa TiO_2 P25 particles were used to thermally coat silica gel granules. A mixture of 4 g TiO_2 and 200 mL distilled water was sonicated for 20 minutes in an ultrasound device (Model 75T, VWR, Mississauga, Ontario). 250 g silica gel was then added to the TiO_2–water mixture. The combined mixture was sonicated for another 20 min. The mixture was then heated using a hot plate to evaporate most of the water and turned into a paste. The paste was subsequently dried in an oven at 100 °C for 2 h and then cured at 500 °C in a furnace for 24 h. After heating, coated silica gel was washed with distilled water while shaking vigorously. This was done to remove TiO_2 particles that were not attached firmly to the silica gel support. Washing was repeated several times until the supernatant was free of suspended TiO_2 particles.

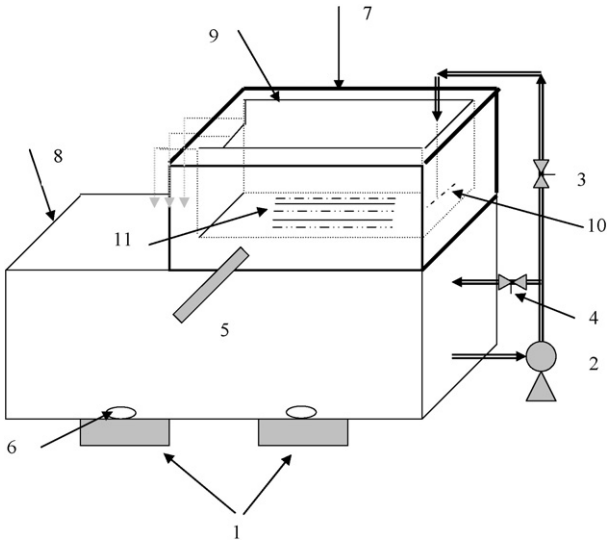

Fig. 1. Experimental set-up: (1) magnetic stirrers, (2) pump, (3) inlet valve, (4) by-pass valve, (5) heater, (6) magnet bars, (7) constant-temperature water bath, (8) liquid feed tank (9) electro-cell, (10) liquid inlet with liquid distributor and (11) electrodes.

2.3. Experimental set-up

2.3.1. Experimental apparatus for the sole electrochemical treatment

A rectangular electro-cell with a height of 5 cm, a width of 20 cm and a length of 25 cm was used for this phase of experimentation (Fig. 1). A schematic diagram of the top view of the electro-cell is shown in Fig. 2. The electro-cell consists of parallel plate electrodes. Three 316-stainless steel anodes and two aluminum cathodes, each of dimensions 18 cm × 5 cm, were used in all experiments. Cathodes and anodes were connected to the negative and positive terminals of a power supply, respectively. The gap between anodes and cathodes was 1.5 cm. The electrolyte was pumped from a liquid holding tank (15-L volume) to the electro-cell via a liquid distributor. The liquid distributor (Fig. 2) was used to spread liquid out evenly at the electro-cell entrance. The electrolyte overflowed a weir at the

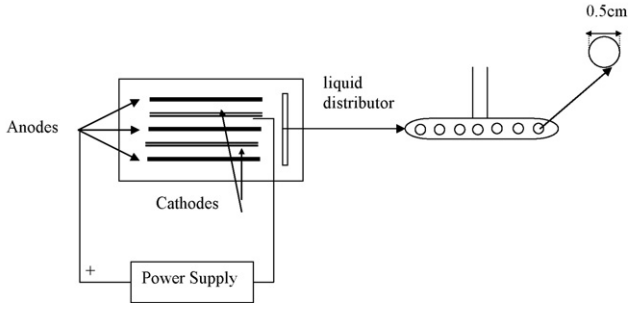

Fig. 2. Schematic diagram of the electro-cell (top view) and details of the liquid distributor.

end of the electro-cell and returned to the holding tank. The electro-cell was placed in a water bath to keep the electrolyte at a constant temperature. Both initial Zn^{++} and Ni^{++} concentrations were 20 ppm. Also, 250 ppm of potassium sulfate was used as a supporting electrolyte.

2.3.2. Experimental apparatus for the sole photocatalytic treatment

For the sole photocatalytic process, a 254 nm UV lamp was placed at the top of the experimental set-up shown in Fig. 1. Electrodes were removed in these experiments. The effects of pH and liquid flow rate on the photodegradtion of LAS were examined using suspended TiO_2 at a concentration of $1\,g\,L^{-1}$. In all experiments, the solution containing TiO_2 was allowed to equilibrate in the darkness for 1 h. Liquid was recirculated in the same mode as that used for the sole electrochemical treatment. In experiments with immobilized TiO_2, a layer of coated silica gel was uniformly placed at the bottom of the reactor. The distance between the UV lamp and coated silica gel particles was 10 cm.

2.3.3. Experimental set-up for combined electrochemical & photocatalytic process

In experiments for the simultaneous removal of metal ions and photocatalytic degradation of LAS, the same experimental set-up as shown in Figs. 1 and 2 was used with the UV lamp placed on the top of the electro-cell. 6 L of a solution containing metal ions (20 ppm), supporting electrolyte (250 ppm) and LAS (100 ppm) was used in these experiments.

3. Results and discussion

3.1. Sole electrochemical removal of metal ions

In an electro-cell, the electrodes reactions are key factors determining the rate of the electrodeposition of metal ions. Dependent on the solution composition, different reactions can occur at the electrodes of an electro-cell. In the present study, following reactions may take place within the electro-cell:

(1) Direct electrodeposition of metal cations at the cathode [7]:

$$Zn^{++}(aq) + 2e^- \Leftrightarrow Zn(s) \qquad E^o = -0.76\,V \qquad (R1)$$

$$Ni^{++}(aq) + 2e^- \Leftrightarrow Ni(s) \qquad E^o = -0.23\,V \qquad (R2)$$

(2) Side reactions such as water decomposition, oxygen reduction and hydrogen evolution at the cathode [8]:

$$2H_2O + 2e^- \Leftrightarrow H_2 + 2OH^- \qquad E^o = -0.83\,V \qquad (R3)$$

$$O_2 + 4H^+ + 4e^- \Leftrightarrow 2H_2O \qquad E^o = +1.23\,V \qquad (R4)$$

$$2H^+ + 2e^- \Leftrightarrow H_2 \qquad (E^o = 0.00\,V) \qquad (R5)$$

(3) The electrolysis of water at the anode under neutral and acidic conditions [8]:

$$H_2O \Leftrightarrow \tfrac{1}{2}O_2 + 2H^+ + 2e^- \qquad (E^o = -1.23\,V) \qquad (R6)$$

Water decomposition, oxygen reduction and hydrogen evolution reactions tend to increase pH at the cathode surface by either H^+ consumption by reactions (R4) and (R5) or OH^- generation by reaction (R3). On the other hand, water hydrolysis at the anode produces H^+ (R6) and thereby may counteract the pH increase caused by the side reactions at the cathode. However, electrolysis of water by reaction (R6) would be the least favorable due to its highest negative standard half-cell potential, E^o, of all above reactions.

By comparing the standard half-cell potentials of the side reactions with those of Zn^{++} and Ni^{++}, one can expect that oxygen reduction occurs preferentially. However, oxygen reduction involves the transfer of four electrons and four H^+ ions. Thus, the overpotential required for this reaction is high. Furthermore, this reaction kinetics is low [9]. Therefore, oxygen reduction is not expected to be a predominant side reaction at the cathode.

Several researchers have reported that H^+ reduction at the cathode occurred under a more negative overpotential than its neutral standard potential. The overpotential for H^+ reduction was observed to be dependent on different factors, including the current density and the electrode material. For example, mercury, lead and aluminum require an overpotential much greater than the neutral standard potential of H^+ in order to have a significant rate of hydrogen evolution [10,11]. The combined effect of all those side reactions might be the reason for the change of the solution pH over the duration of the experiments as observed in the present study. In addition, the side reactions might also compete with Zn^{++} and Ni^{++} for electrons at the cathode surface as discussed further in the next section.

3.1.1. Effect of current density

The effect of the applied current in a range of $0.166–1.11\,mA\,cm^{-2}$ on the removal of Zn^{++} and Ni^{++} was investigated. The results obtained at a fixed liquid volumetric flux of $0.0172\,m^3\,m^{-2}\,s^{-1}$ showed that the removal of Zn^{++} increased slightly from 82 to 89% when the current density was increased from 0.166 to $1.11\,mA\,cm^{-2}$. On the other hand, nickel deposition decreased significantly from 48% to about 10% as shown in Fig. 3. Within the range of current densities used in the present study, the combined amount of both metal ions removed was highest at the current density of $0.166\,mA\,cm^{-2}$. An 82% removal for Zn^{++} and a 48% removal for Ni^{++} were obtained at this current density. In order to ensure that in the sole electrochemical experiments the metal removal was due to electrodeposition only, control measurements were done with the electrolyte solution recirculated in the electro-cell without an applied current. It was found that there was no metal removal (no changes in the metal concentration in the water sample with the run time) under the condition of zero current density. The decreasing trend in nickel deposition with current density are in agreement with the reported literature for Zn-Ni alloy electrodeposition, in which lower percentages of nickel in the deposit were obtained with higher current densities [12,13]. Decreases in the percentage of nickel in the Zn-Ni alloy deposit with increases in the cathode potential were also reported [14].

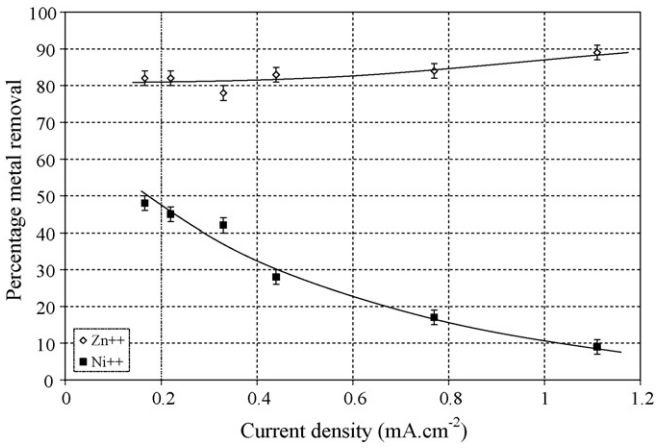

Fig. 3. Effect of current density on the removal of Zn^{++} and Ni^{++}, no pH control, initial metal concentration $[Ni^{++}]_o = [Zn^{++}]_o = 20$ ppm, $T = 25\,^{\circ}C$, $Q = 0.0172\,m^3\,m^{-2}\,s^{-1}$.

The standard half-cell potential of Zn^{++} is -0.76 V, which is higher than that of Ni^{++} (-0.23 V). This implies that Ni^{++} should be reduced more readily than Zn^{++}. However, the results obtained showed that Zn^{++} was actually removed to a greater extent than Ni^{++}. This is known as an anomalous co-deposition, where the less noble metal (Zn^{++} in this case) is preferentially deposited instead of the more noble metal (Ni^{++}) [11]. Zn^{++} has also been reported to preferentially deposit from solutions containing Zn-Co and Zn-Fe ions. Anomalous co-deposition was also encountered in the electroplating of Fe-Ni alloys [15,16]. It was shown, as an example, that in order to achieve a Ni/Fe ratio of 4:1 in the deposit, it was necessary to have an 80:1 molar Ni/Fe ratio in the solution [16].

In general, the side reactions at the cathode ((R3), (R4) and (R5)) would be more favorable at higher current densities [9–11]. These reactions would cause an increase in the solution pH and a decrease in metal deposition since these reactions consumed H^+ and electrons, and produced OH^-. This would lead to a competition for electrons between metal ions and the reactants of theses side reactions at the cathode. This was indeed a case. In the present study, at the highest current density of 1.11 mA cm^{-2}, the solution pH increased from 5.6 initially to 6.5 at the end of the experiment. This indicates that H^+ was reduced by the side reactions at the cathode surface, which also consumed electrons. Consequently, a substantial decrease in Ni^{++} deposition was observed due to more competition for electrons at the cathode surface. Nevertheless, the removal of Zn^{++} still increased slightly since it deposited in the form of zinc hydroxyl. On the other hand, at the lowest current density of 0.167 mA cm^{-2}, the solution pH decreased slightly from the initial value of 5.6–5.0 at the end of the experiment, indicating a very low level of side reactions at the cathode. Therefore, the competition for electrons at the cathode was insignificant. Consequently, more metal ions were deposited at the cathode.

By increasing current density, the rate of hydrogen evolution at the cathode increased. The local pH at the cathode surface thereby increased, resulting in the formation of zinc hydroxide at the cathode surface. However, nickel remained in its ionic form since the electrolyte was buffered by the hydrolysis of Zn^{+2} ions (to form zinc hydroxide) at a pH that was much lower than the required pH for nickel hydroxide formation. Therefore, the deposition of Ni^{++} was suppressed by zinc hydroxide deposited on the cathode surface [17]. This might contribute to the substantial decrease in the removal of Ni^{++} when the current density was increased as shown in Fig. 3.

The overall current efficiency, which was defined as the percentage of the total amount of the electric current applied to the electro-cell to the portion of the current actually used up in the metal deposition at the cathode, decreased by 23% with increases in the current density from 0.166 to 1.11 mA cm^{-2}. At higher current densities, the reduction of hydrogen ions would become significant, and hence, compete with metal ions for free electrons at the cathode surface. The current efficiency for metal ion deposition fell rapidly with time due to hydrogen generation. In the present study, a current efficiency of 22% was obtained at the lowest current density of 0.166 mA cm^{-2}. The low current efficiency was probably due to the low concentrations of Zn^{++} and Ni^{++} used in the present study.

3.1.2. *Effect of the volumetric liquid flux*

Varied liquid rates from 0.0021 to 0.017 $m^3\,m^{-2}\,s^{-1}$ were used to examine the effect of the liquid rate on the removal of Zn^{++} and Ni^{++}. The results obtained are plotted in Fig. 4. Over 47 h of treatment the percentage removal of Zn^{++} increased substantially from 64 to 82% with increases in the liquid rate from 0.0021 to 0.017 $m^3\,m^{-2}\,s^{-1}$ under a fixed current density of 0.166 mA cm^{-2}. Mass transfer of metal ions from the bulk liquid to the cathodes increased with liquid velocity, resulting in a higher Zn^{++} removal. However, the percentage removal of Ni^{++} only increased slightly from 45 to 48% due to competition with Zn^{++} for electrons at the cathode.

In the present study, the variation of the metal ion concentration with the treatment time exhibited an exponential decay, indicating that the removal of metal ions followed a first-order kinetics that can be expressed as [18]:

$$r = \frac{dC_M}{dt} = -k \cdot C_M \quad (1)$$

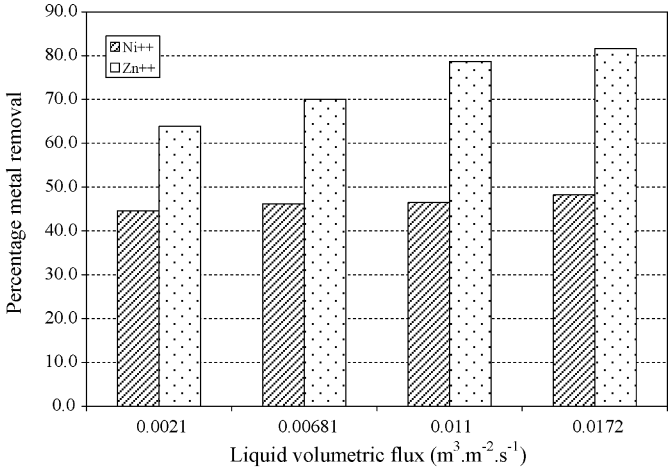

Fig. 4. Effect of liquid flow rate on the removal of Zn^{++} and Ni^{++}, current density = 0.166 mA cm^{-2}, $[Ni^{++}]_o = [Zn^{++}]_o = 20$ ppm, $T = 25\,^{\circ}C$.

Integration of Eq. (1) gives:

$$\ln\left[\frac{C_M}{C_o}\right] = k \cdot t \tag{2}$$

where C_M is the concentration of metal ions remaining in the solution at a given time, k is the first-order metal removal rate constant and r is the metal removal rate. Therefore, as indicated by Eq. (2), the removal rate constant, k, can be obtained from the slope of a semi-log plot of the normalized metal concentration (ratio of the metal concentration at a given time to the initial concentration, C_M/C_{Mo}) versus the treatment time.

The mass transfer rate of metal ions from the bulk liquid to the cathode can be written in a standard rate equation for the mass transfer of a species in a fluid stream to a flat plate as [19]:

$$r_m = k_c \cdot A \cdot (C_M - C_S) \tag{3}$$

where the metal ion concentration, C_S, at the surface of the cathode can be assumed to be zero since the metal deposition is a very fast reaction, k_c is the mass transfer coefficient and A the cathode surface area.

From Eqs. (1) and (3) the average mass transfer coefficient, k_c ($k_c = k \cdot V/A$) can be obtained and presented in Fig. 5. As can be seen in Fig. 5, the removal rate constant increased about 15% and 68% for Ni^{++} and Zn^{++}, respectively, when the liquid rate was increased from 0.0021 to 0.017 $m^3\,m^{-2}\,s^{-1}$. The rate constants obtained in the present study with a rectangular electro-cell are comparable to the rate constants of 0.0201 and 0.0365 h^{-1} for Ni^{++} and Zn^{++}, respectively, obtained at a liquid rate of 0.0137 $m^3\,m^{-2}\,s^{-1}$ in our previous study using a cylindrical flow-through cell with porous electrodes [18]. However, the mass transfer coefficients for Ni^{++} and Zn^{++} in the present study are higher than those with porous electrodes. In the previous study, the deficiency in mass transfer was made up by the higher surface area of the porous electrodes (total surface area = 1760 cm^2) compared to that of the flat electrodes in the present study (total surface area = 360 cm^2). As a result, the removal rate constant and the percentage removal are comparable between the two cases.

For data generalization, the dimensionless J_D factor for mass transfer is often used. It can be handy for estimations of the mass transfer coefficients used in design or performance evaluation of large-scale systems. The J_D factor is defined as [20]:

$$J_D = \frac{Sh}{Re \cdot Sc^{1/3}} = \frac{k_c \cdot L/D_{AB}}{Re \cdot Sc^{1/3}} \tag{4}$$

where k_c is the mass transfer coefficient, L is the characteristic length (in the present study, it is the hydraulic diameter of the opened-channel electro-cell, $L = 0.086$ m), D_{AB} is the diffusivity of the metal ion in liquid, Re is the Reynolds number ($Re = [L \cdot \rho \cdot u]/\mu$; u is the fluid superficial velocity, μ and ρ are fluid viscosity and density), Sc is the Schmidt number ($Sc = \mu/[\rho \cdot D_{AB}]$) and Sh is the Sherwood number for mass transfer ($Sh = [k_c \cdot L]/D_{AB}$). D_{AB} values used for Zn^{++} and Ni^{++} were 7.02×10^{-10} $m^2\,s^{-1}$ and 6.13×10^{-10} $m^2\,s^{-1}$, respectively [21]. The Schmidt number $Sc = 1425$ for Zn^{++} and 1631 for Ni^{++}. The Sherwood number ranges from 319 to 535 and 210 to 242 for Zn^{++} and Ni^{++}, respectively, with the corresponding Reynolds numbers from 181 to 1479.

From the experimental data, the values of J_D were calculated and plotted against the Reynolds number in Fig. 6. Correlations for the J_D factors were obtained with the coefficient of determination, r^2, in the order of 0.99 as below:

For Zn^{++}:

$$J_D = 7.68 \cdot Re^{-0.75} \tag{5}$$

and for Ni^{++}:

$$J_D = 12.7 \cdot Re^{-0.94} \tag{6}$$

By equating Eqs. (4) and (5) and rearranging the resultant equation with Re placed in one side of the equation, one can see that the mass transfer coefficient, k_c, for Zn^{++} is proportional to the Reynolds number, hence, the liquid velocity in the electrochemical cell to the exponent of 0.25. Similarly, by combining Eqs. (4) and (6), the mass transfer coefficient for Ni^{++} appears to be independent of liquid velocity ($k_c \propto u^{0.06}$). It is well known that mass transfer coefficient should increase with liquid velocity. However, the removal of Ni^{++} changed insignificantly with

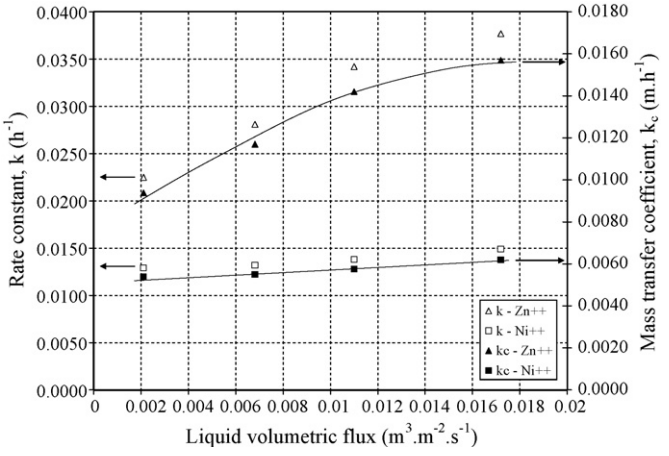

Fig. 5. Variation of the rate constant, k, and the mass transfer coefficient, k_c, of metal ions with liquid volumetric flux in the electro-cell.

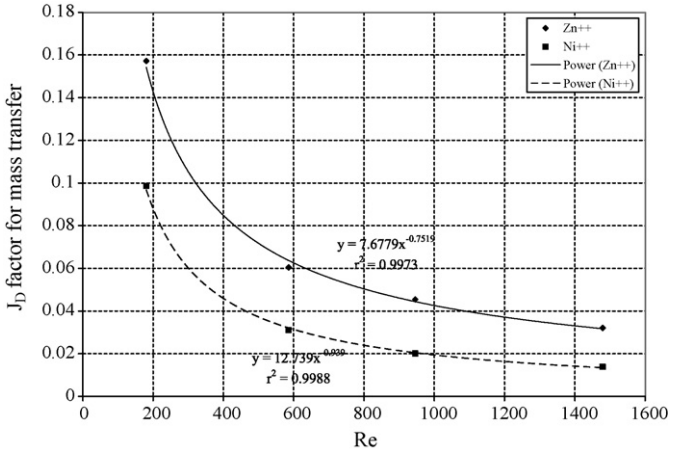

Fig. 6. J_D factor versus the Reynolds numbers for Zn^{++} and Ni^{++} in the electro-cell.

liquid rate due to the deposition anomaly and competition of Zn^{++} for electrons at the cathode surface, as can be seen in Fig. 4. This suggests that the removal of Ni^{++} was predominantly controlled by the reaction at the cathode surface rather than the mass transfer of Ni^{++} from the bulk liquid to the cathode.

3.2. Dark adsorption of LAS and metal ions on TiO_2 surface

In order to determine if any loss of LAS was due to adsorption to the surface of TiO_2 particles or the experimental set-up, a dark experiment was conducted with suspended TiO_2 in liquid. In the dark experiment, a solution of LAS was recirculated inside the system without UV light for 7 h. An 18% reduction in the concentration of LAS was observed in the first hour of dark adsorption. No further reduction of LAS concentration after the first hour was observed. As a result, in order to eliminate the LAS reduction due to adsorption, the solution of LAS and TiO_2 was mixed thoroughly for one hour before starting photocatalytic experiments. Also, this stabilizing period would allow the system to reach a desirable temperature by either adjusting the heater or the cooling water flow rate into the cooling system. Water sampling was started exactly after the stabilizing period and the corresponding concentration was accounted as the initial concentration of LAS at time zero.

Since a substantial amount of foam was generated during the course of an experiment, it was thought that the concentration of LAS in solution might decrease due to foaming. Thus, a dark experiment was also conducted without TiO_2 particles for a 7-h period. The concentrations of LAS did not change significantly over the duration of the experiment.

Adsorption of metal ions on TiO_2 particles was also assessed. The amount of metal ions adsorbed on the surface of suspended TiO_2 particles was measured periodically over 7 h in another dark experiment. Concentrations of Zn^{++} and Ni^{++} decreased by 15% and 8%, respectively, in the first hour and leveled off thereafter. This is in line with reported literature where a 16% removal of Zn^{++} was attributed to adsorption on TiO_2 surface [22]. Also, it has been reported that Zn^{++} adsorption increased in the presence of organic compounds [23].

3.3. Photocatalytic oxidation of LAS by suspended TiO_2

To examine the effect of pH on LAS degradation, the solution pH was varied between 2.0 and 12.0 among various experiments. In each experiment, the solution pH was kept constant by adding an appropriate amount of NaOH (1N) or H_2SO_4 (1N) to the solution during a 7-h period. For experiment without pH control, the pH of the solution dropped from the initial value of 6.4–4.5 at the end of 7 h. The reduction in pH during experiment without pH control could be due to the generation of acidic intermediates in solution. Some intermediates, such as peroxides, alcohols, aldehydes and carboxylic acid, were generated during the photodegradation of DBS [4].

Fig. 7 shows the percentage removal of LAS at varied pH values. The highest percentage removal of 60% was obtained at the pH of about 5.0 as compared with those at very acidic, neutral or basic conditions. It is relevant to note that the zero-point-of-charge pH, pH_{zpc}, for TiO_2 P25 is 6.25 at which the surface of TiO_2 is neutral. Under the neutral condition at pH 6.25, the predominant surface group is TiOH [24,25]. In addition, TiO_2 P25 is known to have an amphoteric character in an aqueous medium. The surface hydroxyl groups, TiOH, undergo different acid–base reactions dependent on the pH value of the medium. Consequently, they are either positively or negatively charged. The adsorption of the substrate and the degradation rate are thus affected by the pH of the aqueous media. At pH above pH_{zpc}, the surface has a net negative charge due to the presence of a substantial amount of TiO^- on the surface of the of TiO_2 particles. On the other hand, at pH below pH_{zpc}, the TiO_2 surface accumulates a net positive charge due to a significant fraction of $TiOH_2^+$ present on the TiO_2 surface. The positive charge on the TiO_2 surface is attractive to the anionic surfactant (LAS). Anionic surfactants, which have electron-rich groups such as sulfonate or sulfate, are thus easily photodegradable [24,26].

Results shown in Fig. 7 indicate that at $pH > pH_{zpc}$, electrostatic repulsion made the adsorption of anionic surfactant molecules to TiO_2 particles more difficult; hence, the degradation of LAS was reduced. The highest rate of LAS degradation is obtained at pH around 5.0, which is less than pH_{zpc}. However, at $pH < 5$, sulfate ions (SO_4^{2-}) from dissociation of the added acid used to adjust the solution pH might compete with LAS for adsorption sites on the surface of TiO_2 particles. Therefore, the rate of LAS decomposition decreased. Similar effect of sulfate ions on the photodegradation of organic compounds by TiO_2 has been reported in the literature [27,28].

The COD of water samples were also measured. Over 7 h at pH about 5.0, a 44% COD removal was observed while a 60% LAS removal was obtained over the same period. This indicates that only 44% of LAS was completely degraded to CO_2 and the rest was converted to intermediates that still consumed oxidants in the COD test, resulting in a lower COD removal. It has been reported that the aromatic group in sodium dodecylbenzene sulfonate was easily decomposed, while the long aliphatic chain (such as one in LAS) was oxidized slowly and partially. Although the complete mineralization of LAS did not occur over a 7-h treatment period, suppression of its surface activity might

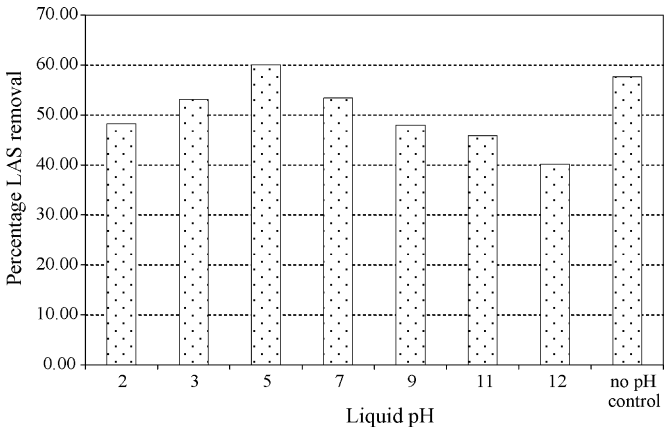

Fig. 7. Effect of pH on the removal of LAS by the sole photocatalytic treatment over 7 h, initial concentration $LAS_o = 100\,mg\,L^{-1}$, $T = 25\,^{\circ}C$, $Q = 0.0172\,m^3\,m^{-2}\,s^{-1}$.

have occurred via either desulfonation or decomposition of the aromatic part since foaming decreased significantly with irradiation time. When LAS was partially cleaved at a certain position, e.g. C-SO_3Na, the remaining intermediate products would be hydrophobic and exhibit no surface activity [4].

Over the duration of the experiment the concentration of LAS exhibited an exponential decay trend with the illumination time. This implies that the removal of LAS by UV/TiO_2 followed first-order kinetics. Generally, the kinetics of heterogeneous photocatalytic reactions is expressed by the Langmuir–Hinshelwood mechanism as below [29]:

$$-\frac{dC}{dt} = \frac{k_r C}{1 + K \cdot C} \quad (7)$$

where k_r is the reaction rate constant and K is the equilibrium constant of adsorption. In a solution with a low concentration C, $K{\cdot}C$ is usually much less than 1 and Eq. (7) is reduced to the first-order kinetic model. This was indeed the case. For all experiments at varied pH from 2.0 to 12.0, the values of k_r were obtained by curve fitting the data to the first-order kinetics model with the coefficient of determination, r^2, range from 0.97 to 0.99. The variation of the rate constant, k_r, with the solution pH is presented in Fig. 8. This again shows that the optimum pH was at 5.0 where the highest k_r was obtained.

3.4. Direct electrochemical oxidation of LAS

Electrochemical oxidation of organic compounds in an aqueous solution may follow two different pathways: direct oxidation at the anode surface and indirect oxidation in the bulk liquid by anodically formed oxidants. Most of electrochemical degradation of organic materials occurred via hydroxyl radicals formed on the anode surface by dissociation of water and/or direct oxidation of hydroxide ions [30]. Hydroxyl radicals have a very short life and either oxidize organics directly or participate in the formation of secondary oxidants such as O_2, H_2O_2 or O_3. These oxidants have a reasonably long life, diffuse into the bulk solution and oxidize organic compounds. However, effective pollutant degradation relies on the direct oxidation by hydroxyl radicals at the anode surface since the secondary oxidants are not able to completely degrade organics to carbon dioxide and water.

In order to determine the amount of LAS could be degraded by electrochemical oxidation, an experiment was performed using the electrochemical cell as shown in Fig. 2. The cell voltage was monitored during the experiment and it decreased from the initial value of 6.5 V to the final value of 5.8 V. A reduction in cell voltage implies that there was some H^+ generation from the dissociation of acidic intermediates in the solution, which caused an increase in the solution conductivity. However, pH increased from an initial value of 5.8 to a final value of 7.4 at the end of a 7-h period. Since the only reducible component in the solution was H^+, hydrogen evolution occurred at the cathodes. The rate of hydrogen evolution might be higher than that of H^+ generation, resulting in a rise of the solution pH. After 7 h of treatment, a 24% removal of LAS by direct electrochemical oxidation was observed while COD removal was 17%. This suggests that electrochemical oxidation of LAS might be due to both direct oxidation and indirect oxidation by secondary oxidants, and hence, produced some intermediates that showed up in the COD test of the treated water sample, resulting in the lower COD removal than the LAS concentration reduction.

3.5. Combined photocatalytic and electrochemical technique

3.5.1. Combined method using suspended TiO_2

A comparison of the sole electrochemical technique, the sole photocatalytic process and the combined method was carried out. The normalized LAS concentration versus the treatment time for the three systems in the absence of metal ions and pH control is plotted in Fig. 9. After 7 h of treatment, 71% LAS degradation was achieved with the combined system compared to 58 and 24% LAS removal for the sole photocatalytic treatment and the sole electrochemical system, respectively. The combination of photocatalytic degradation and anodic oxidation enhanced the overall removal of LAS in the combined system.

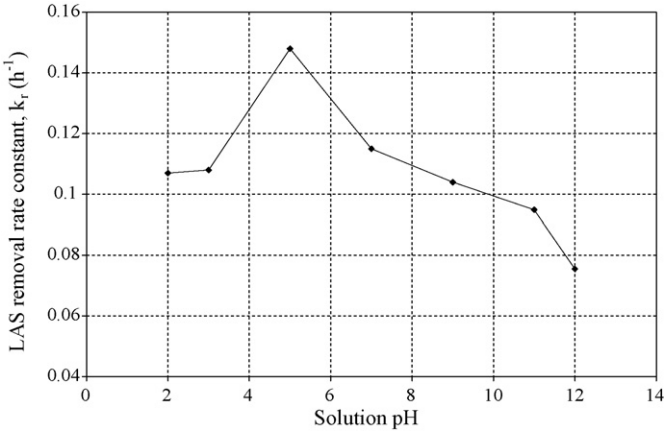

Fig. 8. Variation of the LAS removal rate constant with solution pH.

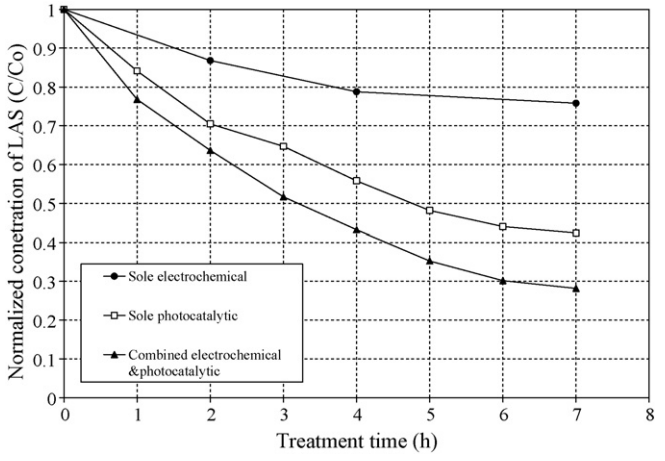

Fig. 9. Comparison of the removal of LAS by different systems: $Q = 0.0172\ m^3\ m^{-2}\ s^{-1}$, $[LAS]_o = 100\ mg\ L^{-1}$, current density = $0.166\ mA\ cm^{-2}$, no pH control, no metal ions.

The effect of the presence of metal ions on LAS degradation using the combined system was also evaluated. It was found that metal ions did not have a significant effect on LAS degradation throughout the duration of the experiment. For the solution containing only LAS, the solution pH increased during 7 h of treatment. Although both electrochemical and photocatalytic oxidations of LAS produced some acidic intermediates, the rate of hydrogen evolution at cathodes appeared to be higher than the rate of H^+ generation from the dissociation of acidic intermediates, resulting in an increase in the solution pH. However, when both metal ions and LAS were present, the solution pH decreased. Metal ions competed with H^+ for electrons and hence hindered hydrogen evolution at the cathode. Consequently, acidic intermediates generated by photocatalytic and electrochemical oxidations of LAS caused a reduction in the solution pH from an initial value of 5.6–4.7 after a 7-h period.

Fig. 10 presents the LAS degradation and the COD removal in the combined system at pH of 5.0 and the case without pH control. A 76% LAS removal was achieved in the experiment with the solution pH maintained at 5.0 as compared with a 68% removal without pH control. Accordingly, the COD removal of 55% and 48% were obtained for cases with and without pH control, respectively. The difference between the percentage of LAS degradation and the COD removal was attributed to the generation of intermediates in the solution. Photocatalytic degradation of LAS was strongly pH dependent. At a pH of 5.0, the surface of TiO_2 particles was positively charged and could easily adsorb the negatively charged anionic surfactant (LAS). As a result, LAS decomposition was better than that of the experiment without pH control, in which the solution pH decreased to more acidic conditions over the duration of the experiment.

In the combined treatment with the presence of LAS and TiO_2 particles, the LAS removal was improved significantly (Fig. 9) while both Zn^{++} and Ni^{++} removal only decreased slightly as compared with that by the sole electrochemical technique in the absence of LAS (Fig. 11). Surfactants could be physically adsorbed to the cathode surface; hence, the effective cathode surface area for the metal deposition might decrease [31]. In addition, since surfactant molecules (LAS) are longer than water molecules, they might hinder the transfer of the metal ions to the cathode-solution interface and the migration of metal ions to the cathode surface to some extent. Therefore, in the presence of LAS, the metal removal at the cathode decreased slightly (equivalent to about 1.5 ppm less metal ions removed). However, the LAS removal was increased substantially from 58% by the sole photocatalytic process to 71% (equivalent to 13 ppm LAS further removed) by the combined method. The significant improvement in the removal of LAS thereby may be considered outweighing the small decrease in the metal removal. In addition, the industrial wastewater of interest contains both LAS and metal ions; and neither the sole electrochemical system nor the sole photocatalytic process could remove both LAS and metal ions efficiently as shown above. Therefore, the combined method can be considered as the best one of all three methods tested in the present study.

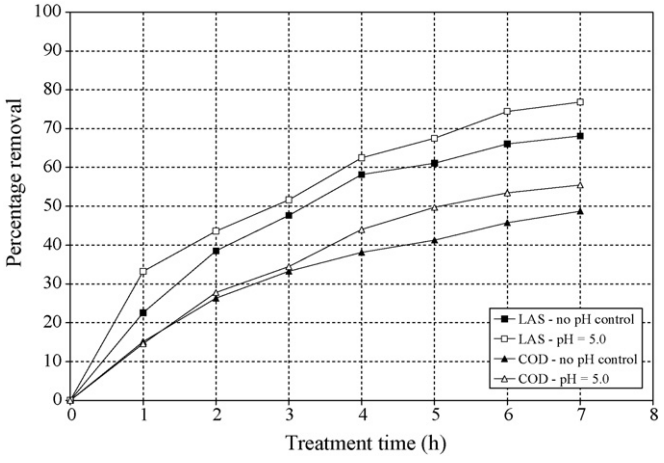

Fig. 10. Effect of pH on the LAS degradation and the COD removal using the combined system. $Q = 0.0172\,m^3\,m^{-2}\,s^{-1}$, $[LAS]_o = 100$ mg/L, $[Ni^{++}]_o = [Zn^{++}]_o = 20$ ppm, current density = $0.166\,mA\,cm^{-2}$.

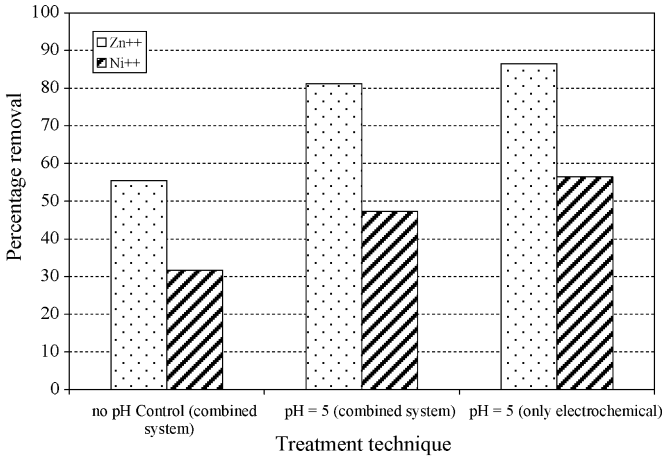

Fig. 11. Comparison of the metal removal by different methods: $Q = 0.0172\,m^3\,m^{-2}\,s^{-1}$, $[LAS]_o = 100\,mg\,L^{-1}$, $[Ni^{++}]_o = [Zn^{++}]_o = 20$ ppm, current density = $0.166\,mA\,cm^{-2}$.

3.5.2. *Photocatalytic degradation of LAS using immobilized TiO_2*

The effectiveness of TiO_2 immobilized on the surface of a silica gel support on LAS degradation was also assessed. A dark experiment was conducted again to quantify the physical adsorption of LAS on the solid surface in the experimental apparatus including silica gel particles. 260 g silica gel granules coated with TiO_2 particles were uniformly placed at the bottom of the reactor in a layer with a thickness of about 2 mm. An equilibrium LAS removal of 19% by dark adsorption was observed after 1 hour. As a result, prior to any photocatalytic experiment, the solution of LAS was recirculated through the reactor in the dark for 1 h. A 31% removal of LAS was obtained with TiO_2 immobilized on silica gel particles. The low LAS degradation could be due to the small ratio the area of the reactor bottom, A, and the total volume of the solution in reactor, V, in the present study. Increases in the A/V ratio would have a significant effect on the removal of organic compounds by immobilized TiO_2 [32].

In order to examine the photoactivity of the immobilized TiO_2, the TiO_2-coated silica gel particles were reused for replica

runs. After each experiment, coated silica gel particles were washed thoroughly with distilled water and dried in air. Dried silica gel particles were then placed at the bottom of the reactor again for experiment replica. There was a small decrease in LAS degradation to 27% for the second and the third runs. This might be due to loss of some TiO_2 particles during experiments and washing of silica gel particles. This could also be due to the saturation of TiO_2 surface with adsorbed intermediates generated by photocatalysis as reported in the literature on the treatment of a phenol solution using TiO_2 immobilized on fiberglass [33].

4. Conclusions

In the present study, simultaneous removal of metal ions and linear alkylbenzene sulfonate in a solution using a combined electrochemical and photocatalytic process was investigated. For comparison purposes, the sole electrochemical removal of Zn^{++} and Ni^{++} and the sole photocatalytic decomposition of LAS were also examined. From the results obtained, the following conclusions were drawn:

For the removal of metal ions by the sole electrochemical technique, the overall current efficiency decreased by 23% with increases in the current density from 0.166 to 1.11 mA cm^{-2}. On the other hand, the removal of Zn^{++} increased about 28% with increases in the liquid rate from 0.00212 to 0.0172 $m^3\ m^{-2}\ s^{-1}$. However, the removal of Ni^{++} did not change significantly with liquid rate.

In the sole photocatalytic system with suspended TiO_2 particles, the optimum pH for LAS degradation was found to be at 5.0. At this pH, 60% of LAS was degraded over a 7-h period. However, for TiO_2 immobilized on silica gel particles, LAS was degraded by only 31% due to a low ratio of the active surface area to the volume of liquid.

In the combined electrochemical–photocatalytic process with suspended TiO_2, the LAS removal was improved by 12% and 19% compared with the sole photocatalytic treatment for the case with pH 5.0 and the case without controlling pH, respectively. The metal removal of 81% for Zn^{++} and 48% for Ni^{++} are comparable to those for the sole electrochemical system. The combined system used in the present study can thus be considered having a great potential in treating industrial effluents containing both heavy metal ions and organic compounds.

Acknowledgement

Financial support from the National Sciences and Engineering Research Council of Canada (NSERC) to the project is greatly appreciated.

References

[1] H.D. Doan, J. Wu, Biological treatment of wastewater from a polymer coating process, J. Chem. Technol. Biotechnol. 77 (2002) 1076–1083.
[2] M.R.V. Lanza, R. Bertazzoli, Removal of Zn(II) from chloride medium using a porous electrode: current penetration within the cathode, J. Appl. Electrochem. 30 (2000) 61–70.
[3] K. Juttner, U. Galla, H. Schmieder, Electrochemical approaches to environmental problems in the process industry, Electrochim. Acta 45 (2000) 2575–2594.
[4] H. Hidaka, H. Kubota, M. Gratzel, E. Pelizzetti, N. Serpone, Photodegradation of surfactants II: degradation of sodium dodecylbenzene sulfonate catalysed by titanium dioxide particles, J. Photochem. 35 (1986) 219–230.
[5] C. Zhang, K.T. Valsaraj, W.D. Constant, D. Roy, Aerobic biodegradation kinetics of four anionic and nonanionic surfactants at sub-and supra-critical micelle concentrations (CMCs), Water Res. 33 (1) (1999) 115–124.
[6] APHA, AWWA, WPCF, Standards Methods for the Examination of Water and Wastewater, twenty-second ed., American Public Health Association, New York, 2000.
[7] G. Prentice, Electrochemical Engineering Principles, Prentice-Hall International, Englewood Cliffs, NJ, 1991.
[8] P. Atkins, L. Jones, Chemistry: Molecules, Matter and Change, third ed., WH Freeman, New York, 1997.
[9] D. Pletcher, F.C. Walsh, Industrial Electrochemistry, second ed., Chapman-Hall, London, 1990.
[10] D.J. Pickett, The analysis of batch electrochemical reactor with continuously recirculating electrolyte, Electrochim. Acta 18 (1973) 835–837.
[11] A. Brenner, Electrodeposition of Alloys. Principles and Practices, vols. 1 and 2, Academic Press, New York, 1963.
[12] A. Abibsi, J.K. Dennis, N.R. Short, The effect of plating variables on zinc-nickel alloy electrodeposition, Trans. Inst. Met. Finish 69 (1991) 145–148.
[13] F.J. Fabri Miranda, O.E. Barcia, S.L. Diaz, O.R. Mattos, R. Wiart, Electrodeposition of Zn-Ni alloys in sulfate electrolytes, Electrochim. Acta 41 (1996) 1041–1049.
[14] G. Roventi, R. Fratesi, R.A. Della Guardia, G. Barucca, Normal and anomalous codeposition of Zn-Ni alloys from chloride bath, J. Appl. Electrochem. 30 (2000) 173–179.
[15] H. Dahms, H. Croll, The anomalous codeposition of iron-nickel alloys, J. Electrochem. Soc. 112 (1965) 771–775.
[16] H. Deligianni, L.T. Romankiw, In situ surface pH measurement during electrolysis using a rotating electrode, IBM J. Res. Develop. 37 (1993) 85–95.
[17] H. Fukushima, T. Akiyama, K. Higashi, R. Kammel, M. Karimkhani, Electrodeposition behavior of Zn-Ni alloys from sulfate baths over a wide range of current density, Metallurgy 42 (1988) 242–247.
[18] H.D. Doan, J. Wu, R. Mitzakov, Combined electrochemical and biological treatment of industrial wastewater using porous electrodes, J. Chem. Technol. Biotechnol. 81 (2006) 1398–1408.
[19] R.B. Bird, W.E. Stewart, E.N. Lightfoot, Transport Phenomena, second ed., John Wiley & Sons, Inc., New York, 2002.
[20] R.E. Treybal, Mass-Transfer Operations, third ed., McGraw-Hill, Inc., New York, 1987.
[21] A. Anderko, M.M. Lenka, Modeling self-diffusion in multicomponent aqueous electrolyte systems in wide concentration ranges, Ind. Eng. Chem. Res. 37 (1998) 2878–2888.
[22] K. Rajeshwar, C.R. Chenthamarakshan, Y. Ming, W. Sun, Cathodic photoprocesses on titania films and in aqueous suspensions, J. Electroanal. Chem. 538–539 (2002) 173–182.
[23] S. Somasundaram, Y. Ming, C.R. Chenthamarakshan, Z.A. Schelly, K. Rajeshwar, Free radical-mediated heterogeneous photocatalytic reduction of metal ions in UV-irradiated titanium dioxide suspensions, J. Phys. Chem. B 108 (2004) 4784–4788.
[24] C. Kormann, D.W. Behnemann, M.R. Hoffmann, Photolysis of chloroform and other organic molecules in aqueous TiO_2 suspensions, Environ. Sci. Technol. 25 (1991) 494–500.
[25] W. Stumm, J.J. Morgan, Aquatic Chemistry, second ed., Wiley Inter-Science, New York, 1981.
[26] H. Hidaka, S. Yamada, S. Suenaga, J. Zhao, N. Serponi, E. Pelezzetti, Photodegardation of surfactants part VI: complete photocatalytic degradation of anionic, cationic and nonionic surfactants in aqueous semiconductor dispersions, J. Mol. Catal. 59 (1990) 279–290.
[27] M. Abdullah, G.K.C. Low, R.W. Matthews, Effects of common inorganic anions on rates of photocatalytic oxidation of organic carbon over illuminated titanium dioxide, J. Phys. Chem. 94 (1990) 6820–6825.

[28] S. Yamazaki, N. Fujinaga, K. Araki, Effect of sulfate ions for sol-gel synthesis of titania photocatalyst, Appl. Catal. A 210 (2001) 97–102.
[29] J.M. Herrmann, Heterogeneous photocatalysis: fundamentals and applications to the removal of various types of aqueous pollutants, Catal. Today 53 (1999) 115–129.
[30] P. Canizares, J.A. Dominguez, M.A. Rodrigo, J. Villasenor, J. Rodriguez, Effect of current intensity in the electrochemical oxidation of aqueous phenol wastes at an activated carbon and steel anode, Ind. Eng. Chem. Res. 38 (1999) 3779–3785.
[31] C.H. Huang, Effect of surfactants on recovery of nickel from nickel plating wastewater by electrowinning, Water Res. 29 (1995) 1821–1826.
[32] R.W. Matthews, Photooxidative degradation of coloured organics in water using supported catalysts TiO_2 on sand, Water Res. 25 (1991) 1169–1176.
[33] V. Brezova, A. Blazkova, M. Breznan, P. Kottas, Phenol degradation on glass fibers with immobilized titanium dioxide particles, Collect. Czech. Chem. Commun. 60 (1995) 788–794.